Localizing the VHE gamma-ray source at the Galactic Centre

Fabio Acero, F. Aharonian, A. G. Akhperjanian, G. Anton, U. Barres de Almeida, A. R. Bazer-Bachi, Y. Becherini, B. Behera, K. Bernlöhr, A. Bochow, et al.

Monthly Notices
of the
ROYAL ASTRONOMICAL SOCIETY

Mon. Not. R. Astron. Soc. **402,** 1877–1882 (2010) doi:10.1111/j.1365-2966.2009.16014.x

Localizing the VHE γ-ray source at the Galactic Centre

HESS Collaboration F. Acero,[1] F. Aharonian,[2,3] A. G. Akhperjanian,[4] G. Anton,[5] U. Barres de Almeida,[6⋆] A. R. Bazer-Bachi,[7] Y. Becherini,[8] B. Behera,[9] K. Bernlöhr,[10,2] A. Bochow,[2] C. Boisson,[11] J. Bolmont,[12] V. Borrel,[7] I. Braun,[2] J. Brucker,[5] F. Brun,[12] P. Brun,[13] R. Bühler,[2] T. Bulik,[14] I. Büsching,[15] T. Boutelier,[16] P. M. Chadwick,[6] A. Charbonnier,[12] R. C. G. Chaves,[2] A. Cheesebrough,[6] J. Conrad,[17] L.-M. Chounet,[18] A. C. Clapson,[2] G. Coignet,[19] M. Dalton,[10] M. K. Daniel,[6] I. D. Davids,[20,15] B. Degrange,[18] C. Deil,[2] H. J. Dickinson,[6] A. Djannati-Ataï,[8] W. Domainko,[2] L. O'C. Drury,[3] F. Dubois,[19] G. Dubus,[16] J. Dyks,[21] M. Dyrda,[22] K. Egberts,[2] P. Eger,[5] P. Espigat,[8] L. Fallon,[3] C. Farnier,[1] S. Fegan,[18] F. Feinstein,[1] A. Fiasson,[19] A. Förster,[2] G. Fontaine,[18] M. Füßling,[10] S. Gabici,[3] Y. A. Gallant,[1] L. Gérard,[8] D. Gerbig,[23] B. Giebels,[18] J. F. Glicenstein,[13] B. Glück,[5] P. Goret,[13] D. Göring,[5] M. Hauser,[9] S. Heinz,[5] G. Heinzelmann,[24] G. Henri,[16] G. Hermann,[2] J. A. Hinton,[25] A. Hoffmann,[26] W. Hofmann,[2] P. Hofverberg,[2] M. Holleran,[15] S. Hoppe,[2] D. Horns,[24] A. Jacholkowska,[12] O. C. de Jager,[15] C. Jahn,[5] I. Jung,[5] K. Katarzyński,[27] U. Katz,[5] S. Kaufmann,[9] M. Kerschhaggl,[10] D. Khangulyan,[2] B. Khélifi,[18] D. Keogh,[6] D. Klochkov,[26] W. Kluźniak,[21] T. Kneiske,[24] Nu. Komin,[13] K. Kosack,[2] R. Kossakowski,[19] G. Lamanna,[19] J.-P. Lenain,[11] T. Lohse,[10] V. Marandon,[8] O. Martineau-Huynh,[12] A. Marcowith,[1] J. Masbou,[19] D. Maurin,[12] T. J. L. McComb,[6] M. C. Medina,[11] J. Méhault,[1] R. Moderski,[21] E. Moulin,[13] M. Naumann-Godo,[18] M. de Naurois,[12] D. Nedbal,[28] D. Nekrassov,[2] B. Nicholas,[29] J. Niemiec,[22] S. J. Nolan,[6] S. Ohm,[2] J-F. Olive,[7] E. de Oña Wilhelmi,[2] K. J. Orford,[6] M. Ostrowski,[30] M. Panter,[5] M. Paz Arribas,[10] G. Pedaletti,[9] G. Pelletier,[16] P.-O. Petrucci,[16] S. Pita,[8] G. Pühlhofer,[26] M. Punch,[8] A. Quirrenbach,[9] B. C. Raubenheimer,[15] M. Raue,[31,2] S. M. Rayner,[6] O. Reimer,[32] M. Renaud,[8] F. Rieger,[31,2] J. Ripken,[17] L. Rob,[26] S. Rosier-Lees,[19] G. Rowell,[29] B. Rudak,[21] C. B. Rulten,[6] J. Ruppel,[23] F. Ryde,[33] V. Sahakian,[4] A. Santangelo,[26] R. Schlickeiser,[23] F. M. Schöck,[5] A. Schönwald,[10] U. Schwanke,[10] S. Schwarzburg,[26] S. Schwemmer,[9] A. Shalchi,[23] M. Sikora,[21] J. L. Skilton,[25] H. Sol,[11] Ł. Stawarz,[30] R. Steenkamp,[20] C. Stegmann,[5] F. Stinzing,[5] G. Superina,[18] I. Sushch,[10] A. Szostek,[30,16] P. H. Tam,[9] J.-P. Tavernet,[12] R. Terrier,[8] O. Tibolla,[2] M. Tluczykont,[24] C. van Eldik,[2†] G. Vasileiadis,[1] C. Venter,[15] L. Venter,[11] J. P. Vialle,[19] P. Vincent,[12] M. Vivier,[13] H. J. Völk,[2] F. Volpe,[2] S. J. Wagner,[9] M. Ward,[6] A. A. Zdziarski[21] and A. Zech[11]

[1] *Laboratoire de Physique Théorique et Astroparticules, Université Montpellier 2, CNRS/IN2P3, CC 70, Place Eugène Bataillon, F-34095 Montpellier Cedex 5, France*

⋆Supported by CAPES Foundation, Ministry of Education of Brazil.
†E-mail: Christopher.van.Eldik@mpi-hd.mpg.de
‡UMR 7164 (CNRS, Université Paris VII, CEA, Observatoire de Paris).

[2]*Max-Planck-Institut für Kernphysik, PO Box 103980, D 69029 Heidelberg, Germany*
[3]*Dublin Institute for Advanced Studies, 5 Merrion Square, Dublin 2, Ireland*
[4]*Yerevan Physics Institute, 2 Alikhanian Brothers St., 375036 Yerevan, Armenia*
[5]*Universität Erlangen-Nürnberg, Physikalisches Institut, Erwin-Rommel-Str. 1, D 91058 Erlangen, Germany*
[6]*Department of Physics, University of Durham, South Road, Durham DH1 3LE*
[7]*Centre d'Etude Spatiale des Rayonnements, CNRS/UPS, 9 av. du Colonel Roche, BP 4346, F-31029 Toulouse Cedex 4, France*
[8]*Astroparticule et Cosmologie (APC), CNRS, Universite Paris 7 Denis Diderot, 10, rue Alice Domon et Leonie Duquet, F-75205 Paris Cedex 13, France*‡
[9]*Landessternwarte, Universität Heidelberg, Königstuhl, D 69117 Heidelberg, Germany*
[10]*Institut für Physik, Humboldt-Universität zu Berlin, Newtonstr. 15, D 12489 Berlin, Germany*
[11]*LUTH, Observatoire de Paris, CNRS, Université Paris Diderot, 5 Place Jules Janssen, 92190 Meudon, France*
[12]*LPNHE, Université Pierre et Marie Curie Paris 6, Université Denis Diderot Paris 7, CNRS/IN2P3, 4 Place Jussieu, F-75252 Paris Cedex 5, France*
[13]*IRFU/DSM/CEA, CE Saclay, F-91191 Gif-sur-Yvette, Cedex, France*
[14]*Astronomical Observatory, The University of Warsaw, Al. Ujazdowskie 4, 00-478 Warsaw, Poland*
[15]*Unit for Space Physics, North-West University, Potchefstroom 2520, South Africa*
[16]*Laboratoire d'Astrophysique de Grenoble, INSU/CNRS, Université Joseph Fourier, BP 53, F-38041 Grenoble Cedex 9, France*
[17]*Oskar Klein Centre, Department of Physics, Stockholm University, Albanova University Center, SE-10691 Stockholm, Sweden*
[18]*Laboratoire Leprince-Ringuet, Ecole Polytechnique, CNRS/IN2P3, F-91128 Palaiseau, France*
[19]*Laboratoire d'Annecy-le-Vieux de Physique des Particules, Université de Savoie, CNRS/IN2P3, F-74941 Annecy-le-Vieux, France*
[20]*Department of Physics, University of Namibia, Private Bag 13301, Windhoek, Namibia*
[21]*Nicolaus Copernicus Astronomical Center, ul. Bartycka 18, 00-716 Warsaw, Poland*
[22]*Instytut Fizyki Jądrowej PAN, ul. Radzikowskiego 152, 31-342 Kraków, Poland*
[23]*Institut für Theoretische Physik, Lehrstuhl IV: Weltraum und Astrophysik, Ruhr-Universität Bochum, D 44780 Bochum, Germany*
[24]*Universität Hamburg, Institut für Experimentalphysik, Luruper Chaussee 149, D 22761 Hamburg, Germany*
[25]*School of Physics & Astronomy, University of Leeds, Leeds LS2 9JT*
[26]*Institut für Astronomie und Astrophysik, Universität Tübingen, Sand 1, D 72076 Tübingen, Germany*
[27]*Toruń Centre for Astronomy, Nicolaus Copernicus University, ul. Gagarina 11, 87-100 Toruń, Poland*
[28]*Faculty of Mathematics and Physics, Charles University, Institute of Particle and Nuclear Physics, V Holešovičkách 2, 18000 Prague 8, Czech Republic*
[29]*School of Chemistry & Physics, University of Adelaide, Adelaide 5005, Australia*
[30]*Obserwatorium Astronomiczne, Uniwersytet Jagielloński, ul. Orla 171, 30-244 Kraków, Poland*
[31]*European Associated Laboratory for Gamma-Ray Astronomy, jointly supported by CNRS and MPG*
[32]*Institut für Astro- und Teilchenphysik, Leopold-Franzens-Universität Innsbruck, A-6020 Innsbruck, Austria*
[33]*Oskar Klein Centre, Department of Physics, Royal Institute of Technology (KTH), Albanova, SE-10691 Stockholm, Sweden*

Accepted 2009 November 9. Received 2009 November 2; in original form 2009 September 21

ABSTRACT

The inner 10 pc of our Galaxy contains many counterpart candidates of the very high energy (VHE; >100 GeV) γ-ray point source HESS J1745−290. Within the point spread function of the H.E.S.S. measurement, at least three objects are capable of accelerating particles to VHE and beyond and of providing the observed γ-ray flux. Previous attempts to address this source confusion were hampered by the fact that the projected distances between these objects were of the order of the error circle radius of the emission centroid (34 arcsec, dominated by the pointing uncertainty of the H.E.S.S. instrument). Here we present H.E.S.S. data of the Galactic Centre region, recorded with an improved control of the instrument pointing compared to H.E.S.S. standard pointing procedures. Stars observed during γ-ray observations by optical guiding cameras mounted on each H.E.S.S. telescope are used for off-line pointing calibration, thereby decreasing the systematic pointing uncertainties from 20 to 6 arcsec per axis. The position of HESS J1745−290 is obtained by fitting a multi-Gaussian profile to the background-subtracted γ-ray count map. A spatial comparison of the best-fitting position of HESS J1745−290 with the position and morphology of candidate counterparts is performed. The position is, within a total error circle radius of 13 arcsec, coincident with the position of the supermassive black hole Sgr A* and the recently discovered pulsar wind nebula candidate G359.95−0.04. It is significantly displaced from the centroid of the supernova remnant Sgr A East, excluding this object with high probability as the dominant source of the VHE γ-ray emission.

Key words: ISM: individual: Sgr A East – ISM: individual: Sgr A* – ISM: individual: G 359.95−0.04 – Galaxy: centre – gamma-rays: observations.

1 VHE γ-RAYS FROM THE GALACTIC CENTRE

Since the discovery of the strong compact radio source Sgr A* (Balick & Brown 1974), the Galactic Centre (GC), as the closest galactic nucleus, has served as a unique laboratory for investigating the astrophysics of galactic nuclei in general. The radio picture (LaRosa et al. 2000) of the central few 100 pc around the centre of the Milky Way exhibits a complex and very active region, with numerous sources of non-thermal radiation, making this region a prime target for observations at very high energies (VHE; >100 GeV). Indeed, several Imaging Atmospheric Cherenkov Telescopes (IACTs) have detected a source of VHE γ-rays in the direction of the GC (Aharonian et al. 2004; Kosack et al. 2004; Tsuchiya et al. 2004; Albert et al. 2006). The H.E.S.S. instrument (see Aharonian et al. 2006a, and references therein) provides the most precise VHE data on this source till date, henceforth called HESS J1745−290. As shown with deep observations in 2004, HESS J1745−290 is a point source for H.E.S.S. (rms spatial extension of <1.2 arcmin at 95 per cent CL) and is within $7'' \pm 14''_{\rm stat} \pm 28''_{\rm sys}$, positionally coincident with the bright radio source Sgr A* (Aharonian et al. 2006b). The measured energy spectrum does not fit dark matter (DM) model spectra – at least for the most popular models of DM annihilation – ruling out the fact that the bulk of the TeV emission can solely be of a DM origin (Aharonian et al. 2006b).

Of all possible astrophysics counterparts, the $3 \times 10^6\,{\rm M}_\odot$ supermassive black hole (SMBH) coincident with the Sgr A* radio position is a compelling candidate. Various models predict VHE emission from this object, produced either close to the SMBH itself (Aharonian & Neronov 2005a), within an $\mathcal{O}(10)$ pc zone around Sgr A* due to the interaction of runaway protons with the ambient medium (Aharonian & Neronov 2005b; Liu et al. 2006; Wang, Lu & Chen 2009) or by electrons accelerated in termination shocks driven by winds emerging from within a couple of Schwarzschild radii (Atoyan & Dermer 2004). Sgr A* is a source of bright and frequent X-ray and infrared flares. Detection of quasi-periodic oscillations (QPOs) on time-scales of 100–2250 s has been claimed (e.g. Baganoff et al. 2001; Genzel et al. 2003; Porquet et al. 2003). Recently, however, observations with the Keck II telescope could not confirm the existence of such QPOs (Meyer et al. 2008). No hint for variability, flaring activity or QPOs has been found in the VHE γ-ray light curve in 93 h live time of H.E.S.S. data collected during the years 2004–2006 (Aharonian et al. 2009). Moreover, during a campaign of simultaneous H.E.S.S. and *Chandra* observations of Sgr A* in 2005, a major X-ray flare of 1600 s duration was observed. Although the X-ray flux increased to ≈9 times the quiescent level, no evidence for flaring activity was detected in the VHE light curve (Aharonian et al. 2008). This result makes it highly unlikely that X-ray and VHE emissions originate from the same source region and puts constraints on models predicting correlated flaring.

Besides Sgr A* and its immediate vicinity, there are at least two other production site candidates for VHE emission. The first one is the radio-bright, shell-like supernova remnant (SNR) Sgr A East, which partially surrounds Sgr A*. SNRs have been shown to be efficient particle accelerators (see e.g. Helder et al. 2009), and the presence of an $\mathcal{O}$ (mG) magnetic field (Yusef-Zadeh et al. 1996) makes Sgr A East a compelling candidate for particle acceleration to VHE (Crocker et al. 2005). The second one is the recently detected pulsar wind nebula (PWN) candidate G359.95−0.04 (Wang, Lu & Gotthelf 2006). Despite its faint X-ray flux, it may plausibly emit TeV γ-rays at an energy flux level compatible with the H.E.S.S. observations (Hinton & Aharonian 2007), assuming that G359.95−0.04 is located at the same distance as Sgr A*.

A firm identification of HESS J1745−290 is particularly hampered by the – compared to radio or X-ray instruments – modest angular resolution of the current generation of Cherenkov telescopes (≤5 arcmin for a single γ-ray at TeV energies), which gives rise to source confusion in this densely populated region of the Galaxy. Adopting a distance of 8.33 kpc to the GC (Gillessen et al. 2009), the H.E.S.S. source size upper limit encloses a region of about 2.9 pc radius. Comparing this number to the projected distance of Sgr A* from the radio maximum of Sgr A East and from the X-ray maximum of G359.95−0.04 (3.7 and 0.4 pc, respectively), it becomes clear that a precise position measurement of the centre of gravity of HESS J1745−290 can help to shed light on the nature of this source.

Although previous H.E.S.S. position measurements have been unprecedentedly precise, the relatively large – compared to statistical errors – systematic errors due to pointing uncertainties of the H.E.S.S. array rendered the identification of the major contributing source of the VHE emission, and especially a clear statement on the role of Sgr A East, difficult. In this paper, a refined measurement of HESS J1745−290's emission centroid is reported. Using improved telescope pointing control, the systematic error of the measurement is decreased by a factor of 3 compared to previous results, and the total error on the centroid position is reduced to 13 arcsec (68 per cent containment radius) compared to 34 arcsec in Aharonian et al. (2006b).

2 ASTROMETRIC POINTING CORRECTIONS

The 12 m mirror dishes of the H.E.S.S. telescopes are supported by altitude/azimuth mounts. During γ-ray observations, all four H.E.S.S. telescopes track the targeted source with a nominal precision of better than a few seconds of arc per axis. However, due to the weight of the mirrors and the Cherenkov cameras, $\mathcal{O}$ (mm) deflections of the 15 m long camera masts and the mirror dishes make astrometric corrections necessary. The H.E.S.S. pointing corrections are based on the assumption that telescope deformations, and hence pointing deviations, are reproducible and depend only on the (alt–az) pointing position. They are of the order of a few minutes of arc and are applied to the recorded events after data have been taken, based on a set of independently recorded calibration data (Gillessen 2004). These *standard pointing corrections*, by default applied to all H.E.S.S. data, provide a localization of point-like γ-ray sources with a systematic pointing error of 20 arcsec per axis.

The analysis presented here improves significantly upon these systematic uncertainties by utilizing optical guiding telescopes mounted on the mirror dish of each H.E.S.S. telescope. Stars within the field of view ($0.^\circ3 \times 0.^\circ5$) of the guiding telescopes are imaged by CCD cameras with a projected pixel size of 2.3 arcsec. The guiding telescope optics is slightly defocused such that the light from each star is imaged on to several CCD pixels, making precise position measurement possible. The positions of recorded stars are then compared to nominal coordinates listed in the *Hipparcos* and *Tycho* star catalogues (Perryman et al. 1997). For the analysis presented here, images were recorded at a rate of about $1\,{\rm min}^{-1}$ and contain typically two to 10 identified stars. Additionally, for each H.E.S.S. telescope, deformations of the Cherenkov camera masts are measured by monitoring eight reference LEDs mounted on the Cherenkov camera body. This is done with the help of CCD cameras installed at the centre of each mirror dish. From the combined information of the two CCD cameras, pointing

corrections are calculated for the individual H.E.S.S. telescope. To correct the direction of each γ-ray, linear interpolation is used between the pointing corrections derived from the individual CCD images. The difference in refraction correction for star light and Cherenkov light from γ-ray showers is taken into account. An absolute calibration of the guiding system is performed at the beginning and end of every moon period: the telescopes are pointed at typically 50 bright stars uniformly distributed in the sky. Images of the stars are recorded with the guiding telescopes. Additionally, the star light is reflected by the mirrors on to screens in front of the Cherenkov cameras, and images of the stars and of the reference LEDs are recorded with the central CCD cameras. From these measurements, altitude- and azimuth-dependent pointing models are derived. These relate, for any given observation position, the star position measured with the guiding telescopes to the star spot position determined with the central CCD camera.

Typically, the *precision pointing corrections* derived in this way differ only slightly from the standard pointing corrections. However, the observation of stars and camera body simultaneously to γ-ray collection reduces systematic uncertainties significantly, such as hysteresis effects observed in the camera mast structure, which limit the precision of the altitude determination. Systematic errors due to an observed long-term movement of the telescope foundations are cancelled, as are uncertainties in the absolute positioning of the tracking system. Thermal expansion of the CCD chips due to changes in the ambient temperature is accounted for in the precision pointing model. For the data set presented in this analysis, a total systematic pointing error of ± 6 arcsec per axis on the sky was derived (Braun 2007). Possible systematic effects regarding the reconstruction of the γ-ray shower images, such as an inhomogeneous field of view or the effect of Earth's magnetic field on the image parameters, have been studied. No effect was observed that would systematically shift the centroid of point-like γ-ray sources by more than 2 arcsec. Furthermore, the precision pointing corrections were extensively validated on VHE γ-ray data of point-like sources with positions and extensions known from observations at another waveband (with much better pointing accuracy and angular resolution). A detailed description of the precision pointing technique and the estimation of systematic errors are beyond the scope of this paper and will be published elsewhere.

3 ANALYSIS OF γ-RAY DATA

Since the guiding telescopes for precision pointing corrections are in operation only since 2005, the results reported here are based on 64 h (live time) of data recorded with the H.E.S.S. instrument between 2005 May 4 and August 23 and between 2006 April 4 and August 4. Most of the observations (59 h) were carried out in a *wobble mode*, i.e. the telescope pointing direction was offset from the target direction (Sgr A*) by typically $0.^{\circ}5$–$0.^{\circ}7$ in either right ascension or declination, in an alternating fashion. The remaining 5 h of data were recorded with various offsets of up to $1.^{\circ}4$ from the direction of Sgr A*. The mean zenith angle of the data described here is 23° and the observation zenith angles range from 6° to 60°.

Data were analysed with the standard H.E.S.S. calibration and reconstruction chain (Aharonian et al. 2006a). First, each shower image recorded by the Cherenkov cameras was corrected for astrometry using the precision pointing corrections described above. To suppress background events caused by cosmic-ray-induced air showers, γ-rays were selected based on the shape of the shower images in the Cherenkov cameras, as described by Hillas parameters (Hillas 1985) using *hard cuts* (Aharonian et al. 2006a). As opposed to standard cuts, hard cuts select high-intensity shower images, reducing further the number of background events (relative to signal) at the expense of a higher energy threshold ($\approx$630 GeV for a mean zenith angle of 23°). In addition, this high-intensity selection leads to a sample of well-reconstructed showers, resulting in an improved angular resolution. After this event selection, the direction of each γ-ray was reconstructed by intersecting the major axes of the Hillas ellipses, following algorithm 3 from Hofmann et al. (1999). This approach uses the Hillas width and length of the shower images to estimate the γ-ray direction independently with each telescope. These estimates are then combined to yield the optimum γ-ray direction, which improves upon the standard H.E.S.S. reconstruction in terms of angular resolution. Reconstructed events were accumulated in a $2^{\circ} \times 2^{\circ}$ image, centred at the position of Sgr A* and binned into squares of $0.^{\circ}03$ angular size. The remaining background from cosmic-ray-induced showers was estimated using the ring-background technique (Berge, Funk & Hinton 2007), excluding regions containing known γ-ray sources, such as the band of diffuse emission along the GC ridge (Aharonian et al. 2006c). A background subtraction based on a template approach (Rowell 2003) gives consistent results. An excess of 1313 ± 42 VHE γ-rays is found within a circle of a radius of $0.^{\circ}1$ centred on Sgr A*, with a statistical significance of 46 standard deviations above the background. The energy spectrum derived from this reduced data set is compatible with that reported in Aharonian et al. (2009), which was obtained with a different analysis chain.

The point spread function (PSF), reflecting the angular extension of a point source seen by the H.E.S.S. instrument, was modelled using Monte Carlo (MC) γ-ray simulations, taking into account the distributions of zenith angle, offset of the pointing position relative to Sgr A* as well as the energy distribution of γ-rays from HESS J1745−290 (Aharonian et al. 2009). The simulated PSF can be well described by the sum of two Gaussian functions with equal mean (Aharonian et al. 2006a). The overall angular resolution of the data set is 3.9 arcmin (68 per cent containment radius).

4 POSITION OF HESS J1745−290

The centroid of the VHE emission was determined by fitting the acceptance-corrected and background-subtracted γ-ray count map in a window of $\pm 0.^{\circ}2$ centred on Sgr A*, with a two-dimensional radially symmetric profile. The fit model was composed of a double-Gaussian part accounting for the PSF of the H.E.S.S. instrument, convolved with an assumed Gaussian surface brightness distribution to account for a possible intrinsic extension of the source. This source extension and the overall normalization were left as free parameters in the fit. The PSF was fixed from MC simulations as described above.

Diffuse γ-ray emission along the GC ridge introduces an asymmetric γ-ray background in the region of Sgr A*, which could in principle bias the position determination of HESS J1745−290. In a circular region of $0.^{\circ}1$ around the centroid position, this background is at a level of $\approx$15 per cent of the total flux observed from the source (Aharonian et al. 2006b, 2009). In the position determination, the background γ-ray diffuse emission was therefore taken into account by adding an independent term in the fit function with free normalization. The expected diffuse γ-ray emission was modelled – following Aharonian et al. (2006c) – by a radially symmetric Gaussian distribution of a width of $0.^{\circ}8$ centred at the GC, multiplied with the density distribution of molecular clouds in the region from CS line emission measurements (Tsuboi, Handa & Ukita 1999). The position fit is largely insensitive to details of the diffuse

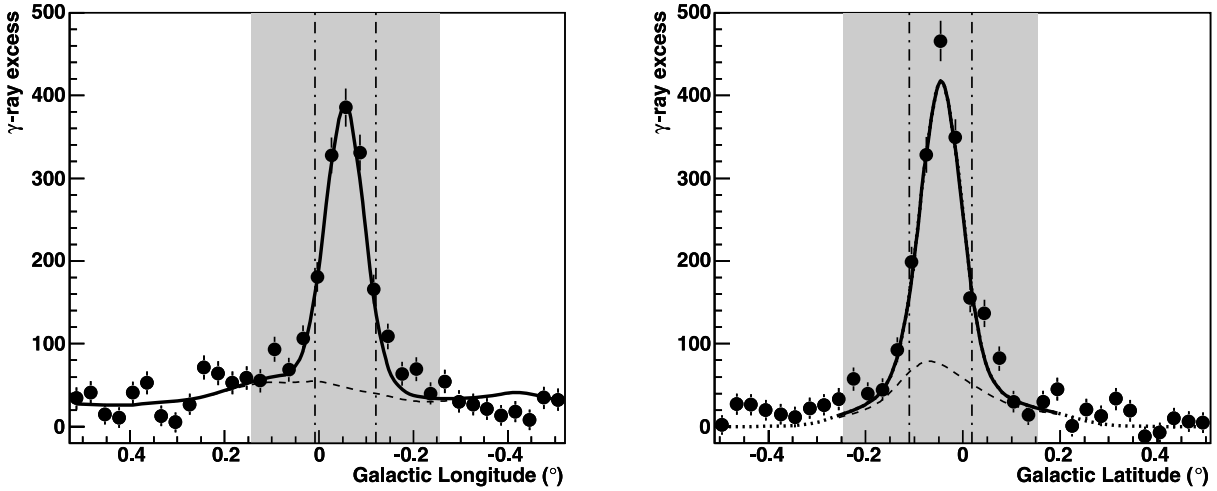

Figure 1. Projections along Galactic longitude (left-hand panel) and Galactic latitude (right-hand panel) of the acceptance-corrected γ-ray excess map and the best-fitting function (solid line). The latitude and longitude ranges used for the projections correspond to the respective fit ranges and are indicated by the shaded regions. The 68 per cent containment region of the PSF of the H.E.S.S. instrument is shown by the dashed–dotted lines. The fitted contribution of the diffuse γ-ray emission is indicated by the dashed curve. The dotted lines in the latitude projection depict the extension of the best-fitting function beyond the latitude coverage of the CS line emission survey used for the diffuse γ-ray background model. Possible features in the γ-ray excess outside of the fit boundaries are under study, but do not affect the position determination.

emission model. Indeed, when fitting the position of HESS J1745−290 without taking into account the diffuse component, the result is still consistent within statistical errors with the final position quoted below.

Using a χ^2-minimization procedure, the best-fitting position of HESS J1745−290 in equatorial coordinates is $\alpha = 17^{\rm h}45^{\rm m}39\overset{\rm s}{.}6 \pm 0\overset{\rm s}{.}4_{\rm stat} \pm 0\overset{\rm s}{.}4_{\rm sys}$, $\delta = -29^\circ 0' 22'' \pm 6''_{\rm stat} \pm 6''_{\rm sys}$ (J2000.0). The best-fitting probability is 12 per cent. The best-fitting position is, within $8'' \pm 9''_{\rm stat} \pm 9''_{\rm sys}$, coincident with the position of Sgr A* and fully compatible with the position reported from the 2004 data set (Aharonian et al. 2006b). Changing the background subtraction technique, the image binning or the fit boundaries did not affect the position by more than 2 arcsec. Assuming a Gaussian distribution of surface brightness, an rms source size upper limit of 1.3 arcmin (95 per cent CL) is derived. The fraction of diffuse emission in a circle of $0\overset{\circ}{.}1$ radius centred on the best-fitting position is 14 per cent, consistent with previous findings (Aharonian et al. 2006b, 2009). Fig. 1 shows longitude and latitude slices of the γ-ray excess map, with the best-fitting function overlaid, to demonstrate the performance of the fit.

5 DISCUSSION

Fig. 2 shows a Very Large Array (VLA) 90 cm image of the innermost 20 pc region of the GC, centred on Sgr A*. The shell-like radio structure of the SNR Sgr A East is clearly visible. The best-fitting position of HESS J1745−290 lies in a region where the radio emission is comparatively low, and is shown as a 68 per cent CL total error contour, computed from the summed (in quadrature) statistical and systematic best-fitting position errors. As can be seen from the figure, the centroid of the VHE source is coincident with the positions of Sgr A* and G359.95−0.04, but inconsistent with the regions of intense radio emission from Sgr A East. Two rather independent approaches to deriving a quantitative statement about the compatibility of HESS J1745−290's best-fitting position with Sgr A East are given in the following.

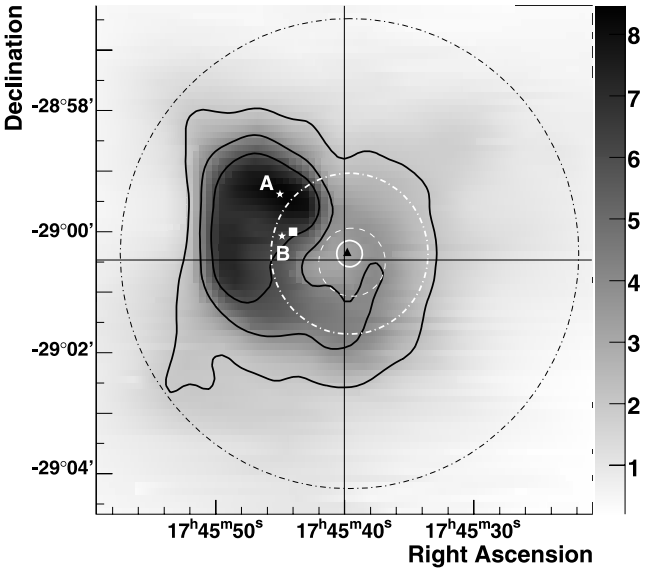

Figure 2. 90 cm VLA radio flux density map (LaRosa et al. 2000) of the innermost 20 pc of the GC, showing emission from the SNR Sgr A East. Black contours denote radio flux levels of 2, 4 and 6 Jy beam^{-1}. The centre of the SNR (Green 2009) is marked by the white square, and the positions of Sgr A* (Reid et al. 1999) and G359.95−0.04 (head position, Wang et al. 2006) are given by the cross hairs and the black triangle, respectively. The 68 per cent CL total error contour of the best-fitting centroid position of HESS J1745−290 is given by the white circle. The dashed white circle shows the same contour for the previously reported H.E.S.S. measurement (Aharonian et al. 2006b). The white and black dashed–dotted lines show the 95 per cent CL upper limit contour of the source extension and the 68 per cent containment region of the H.E.S.S. PSF, respectively. The white stars marked *A* and *B* denote the position of the radio maximum and the best-fitting position for the radio emission after smoothing with the PSF of the H.E.S.S. instrument, respectively.

The white star labelled A in Fig. 2 denotes the position of Sgr A East's radio maximum. Comparing the 68 per cent CL radius of the observed VHE centroid to the angular distance between A and the best-fitting position, a coincidence of the two positions is ruled out with 7.1 standard deviations. By the same arguments, the VHE point emission from the centre of the SNR (Green 2009), indicated as a white square in Fig. 2, is ruled out with 4.7 standard deviations.

Instead of point emission, extended emission can be considered, e.g. by assuming that the hypothetical VHE emission from Sgr A East follows closely the morphology of the radio flux. The centroid of such emission would be detected at the coordinates marked B in Fig. 2. This position was derived by fitting the radio map – smoothed with the H.E.S.S. PSF – with the technique used above for the VHE γ-ray data. Following the methods used for position A, the radio fitting position is 5.4 standard deviations away from the best-fitting VHE centroid position.

The above results are obtained assuming that the VHE emission and radio morphology are correlated. Since the best-fitting position does not coincide with a region of intense radio emission (see Fig. 2), relaxing this assumption leads to more conservative estimates of the association probability. A priori, it would appear conservative to assume that the centroid of TeV emission associated with Sgr A East might appear anywhere within the boundaries, with equal probability. With this assumption one can calculate the probability that the VHE emission is produced inside Sgr A East, but is only by chance positionally coincident with Sgr A* and G359.95−0.04, which themselves are plausible emitters of VHE radiation and thus viable counterpart candidates of HESS J1745−290. Defining the 2 Jy beam^{-1} radio contour of Sgr A East as the SNR boundary, which encloses the best-fitting position of the emission centroid, a chance probability of 9×10^{-5} is derived (corresponding to 3.9 standard deviations). This number slightly changes depending on the assumed size of the SNR boundary. It is clear, however, that even with this conservative approach an association of Sgr A East with the observed VHE γ-ray emission is rather unlikely.

The exclusion of Sgr A East as the main contributor to the VHE emission is a major step towards an identification of HESS J1745−290. Despite the fact that HESS J1745−290 is a non-variable γ-ray source, both G359.95−0.04 and Sgr A* are compelling counterpart candidates, as models exist (see Section 1), which can explain a steady γ-ray flux and variable X-ray emission from Sgr A* at the same time. More information is needed to discriminate between these two objects. Due to their enhanced angular resolution and sensitivity, and their extended energy range, proposed future VHE γ-ray observatories such as CTA or AGIS could shed light on the open question of which of these sources dominates the production of the VHE γ-ray emission from the gravitational centre of our Galaxy.

ACKNOWLEDGMENTS

The support of the Namibian authorities and of the University of Namibia in facilitating the construction and operation of H.E.S.S. is gratefully acknowledged, as is the support by the German Ministry for Education and Research (BMBF), the Max Planck Society, the French Ministry for Research, the CNRS-IN2P3 and the Astroparticle Interdisciplinary Programme of the CNRS, the U.K. Science and Technology Facilities Council (STFC), the IPNP of the Charles University, the Polish Ministry of Science and Higher Education, the South African Department of Science and Technology and National Research Foundation and the University of Namibia. We appreciate the excellent work of the technical support staff in Berlin, Durham, Hamburg, Heidelberg, Palaiseau, Paris, Saclay and Namibia in the construction and operation of the equipment.

REFERENCES

Aharonian F., Neronov A., 2005a, ApJ, 619, 306
Aharonian F., Neronov A., 2005b, Ap&SS, 300, 255
Aharonian F. et al. (H. E. S. S. Collaboration), 2004, A&A, 425, L13
Aharonian F. et al. (H. E. S. S. Collaboration), 2006a, A&A, 457, 899
Aharonian F. et al. (H. E. S. S. Collaboration), 2006b, Phys. Rev. Lett., 97, 221102
Aharonian F. et al. (H. E. S. S. Collaboration), 2006c, Nat, 439, 695
Aharonian F. et al. (H. E. S. S. Collaboration), 2008, A&A, 492, L25
Aharonian F. et al. (H. E. S. S. Collaboration), 2009, A&A, 503, 817
Albert J. et al., 2006, ApJ, 638, L101
Atoyan A., Dermer C. D., 2004, ApJ, 617, L123
Baganoff F. K. et al., 2001, Nat, 413, 45
Balick B., Brown R., 1974, ApJ, 194, 265
Berge D., Funk S., Hinton J., 2007, A&A, 466, 1219
Braun I., 2007, PhD thesis, Univ. Heidelberg
Crocker R. M. et al., 2005, ApJ, 622, 892
Genzel R., Schödel R., Ott T., Eisenhauer F., 2003, Nat, 425, 934
Gillessen S., 2004, PhD thesis, Univ. Heidelberg
Gillessen S., Eisenhauer F., Fritz T. K., Bartko H., Dodds-Eden K., Pfuhl O., Ott T., Genzel R., 2009, ApJ, 692, 1075
Green D. A., 2009, Bull. Astron. Soc. India, 37, 45
Helder E. A. et al., 2009, Sci, 325, 719
Hillas A., 1985, in Jones F. C., ed., Proc. 19th ICRC (La Jolla) Vol. 3. p. 445
Hinton J. A., Aharonian F. A., 2007, ApJ, 657, 302
Hofmann W., Jung I., Konopelko A., Krawczynski H., Lampeitl H., Pühlhofer G., 1999, Astropart. Phys., 122, 135
Kosack K. et al., 2004, ApJ, 608, L97
LaRosa T. N., Kassim N. E., Lazio T. J. W., Hyman S. D., 2000, AJ, 119, 207
Liu S., Melia F., Petrosian V., Fatuzzo M., 2006, AJ, 647, 1099
Meyer L., Do T., Ghez A., Morris M. R., Witzel G., Eckart A., Bélanger G., Schödel R., 2008, AJ, 688, L17
Perryman M. A. C. et al., 1997, A&A, 323, L49
Porquet D., Predehl P., Aschenbach B., Grosso N., Goldwurm A., Goldoni P., Warwick R. S., Decourchelle A., 2003, A&A, 407, L17
Reid M. J., Readhead A. C. S., Vermeulen R. C., Treuhaft R. N., 1999, ApJ, 524, 816
Rowell G. P., 2003, A&A, 410, 389
Tsuboi M., Handa T., Ukita N., 1999, ApJS, 120, 1
Tsuchiya K. et al., 2004, ApJ, 606, L115
Wang Q. D., Lu F. J., Gotthelf E., 2006, MNRAS, 367, 937
Wang Y.-P., Lu Y., Chen L., 2009, Res. Astron. Astrophys., 9, 761
Yusef-Zadeh F., Roberts D. A., Goss W. M., Frail D. A., Green A. J., 1996, ApJ, 466, L25

This paper has been typeset from a TEX/LATEX file prepared by the author.